

# Amperometric Biosensor and Front-End Electronics for Remote Glucose Monitoring by Crosslinked PEDOT-Glucose Oxidase

Yana Aleeva<sup>1</sup>, Giovanni Maira, Michelangelo Scopelliti<sup>2</sup>, Vincenzo Vinciguerra, Graziella Scandurra, Gianluca Cannatà, Gino Giusi<sup>3</sup>, Carmine Ciofi, Viviana Figà, Luigi G. Occhipinti, and Bruno Pignataro

**Abstract**—Focusing on the interplay between interface chemistry, electrochemistry, and integrated electronics, we show a novel low-cost and flexible biosensing platform for continuous glucose monitoring. The amperometric biosensing system features a planar three-electrode structure on a plastic substrate, and a wireless NFC-powered electronic system performing sensor analog front-end, A/D conversion, digital control, and display tasks. The working electrode is made of electropolymerized poly(3,4-ethylenedioxythiophene) film onto a polyethylene terephthalate/gold electrode followed by immobilization of cross-linked glucose oxidase by glutaraldehyde. The advantages offered by such a device, including low-cost materials and instrumentation as well as the good sensitivity of  $9.24 \mu\text{A}/(\text{mM} \cdot \text{cm}^2)$  are promising tools for point-of-care monitoring. It is demonstrated that the devices are good candidates for the development of advanced sensing approaches based on the investigation of the noise produced during operation (fluctuation-enhanced sensing).

**Index Terms**—Amperometric sensors, biosensors, chemical and biological sensors, conductive films, polymer films, remote sensing, thick film biosensors.

Manuscript received January 24, 2018; revised March 30, 2018; accepted April 16, 2018. This work was supported by the Italian MiUR funding through PON R&C 2007-2013—PLAST\_ICs—plastic electronics for smart disposable systems under Grant PON02\_00355-3416798. The associate editor coordinating the review of this paper and approving it for publication was Dr. Chang-Soo Kim. (Corresponding author: Bruno Pignataro.)

Y. Aleeva and G. Maira are with the Dipartimento di Fisica e Chimica, Università degli Studi di Palermo, 90128 Palermo, Italy (e-mail: yana.aleeva@unipa.it; giovanni.maira@gmail.com).

M. Scopelliti is with the Dipartimento di Fisica e Chimica, Università degli Studi di Palermo, 90128 Palermo, Italy, and also with the Consorzio Interuniversitario di Ricerca in Chimica dei Metalli nei Sistemi Biologici, 70121 Bari, Italy (e-mail: michelangelo.scopelliti@unipa.it).

V. Vinciguerra is with STMicroelectronics, 95121 Catania, Italy (e-mail: vincenzo.vinciguerra@st.com).

G. Scandurra, G. Cannatà, G. Giusi, and C. Ciofi are with the Dipartimento di Ingegneria, Università degli Studi di Messina, 98166 Messina, Italy (e-mail: gscandurra@unime.it; gcannata@unime.it; ggiusi@unime.it; cciofi@unime.it).

V. Figà was with the Dipartimento di Fisica e Chimica, Università degli Studi di Palermo, 90128 Palermo, Italy. She is now with the Dipartimento di Ingegneria Industriale, Università degli Studi di Napoli Federico II, 80125 Napoli, Italy (e-mail: viviana\_fg@yahoo.it).

L. G. Occhipinti is with the Electrical Engineering Division, Department of Engineering, University of Cambridge, Cambridge CB3 0FA, U.K. (e-mail: lgo23@cam.ac.uk).

B. Pignataro is with the Dipartimento di Fisica e Chimica, Università degli Studi di Palermo, 90128 Palermo, Italy, and also with the ATen Center, Università degli Studi di Palermo, 90128 Palermo, Italy (e-mail: bruno.pignataro@unipa.it).

Digital Object Identifier 10.1109/JSEN.2018.2831779

## I. INTRODUCTION

THERE are currently about 422 million people with diabetes worldwide as reported by the World Healthcare Organization with more than 80% living in low- and middle-income countries [1]. The increase of diabetes worldwide is leading to the growth in the sales of glucose monitoring devices, which is generating the demand for the global self-monitoring blood glucose devices market. Therefore, the development of flexible, improved, low-cost sensing devices capable of performing glucose measurements in the clinical range will have an enormous impact on a significant portion of the human population for the future generations.

Since the first introduction of continuous glucose monitoring, back in 1974 [2], there is an ever growing interest in cheaper, faster and more reliable monitoring methods.

Electrochemical biosensors have played a major role moving towards Point of care (POC) glucose testing due to their simple measurement principle, the possibility to integrate the full signal processing on a chip, inexpensive instrumentation, and miniaturization [3]–[6]. In addition, flexible plastic electrochemical sensors are promising for wearable and conformable electronics, electronic skin and tissue-integrated sensing as they enable the production of precise sensitive diagnostic devices featured by portability, disposability and low cost. Among them, the amperometric glucose biosensors are poised to play a leading role in continuous blood glucose monitoring owing to its simplicity and easy-to-use methodology [7], [8].

Two critical challenges in the fabrication of plastic amperometric glucose biosensors for wireless-powered systems are: i) the design of suitable enzymatic biosensor interface of the working electrode and ii) the electronic sensor analog front-end (AFE) for electrochemical cell read-out and conditioning of the signal generated by the biosensor amperometrically. As far as the biosensor interface design is concerned, conducting polymers have already been used as electrocatalysts in electrochemical sensors [9]; examples of flexible amperometric glucose biosensors have been demonstrated using paper, cellulose, and polymers [10], [11]. Poly(3,4-ethylenedioxythiophene) (PEDOT) is widely used for glucose sensing applications as it is a biocompatible

conducting polymer and exhibits better stability of its conductivity than polypyrrole [12], [13].

The choice of the enzyme immobilization technique onto the transducer surface is also a crucial step. Methods for enzyme immobilization include physical adsorption, electropolymerization, covalent bonding, entrapment, Langmuir-Blodgett films, layer-by-layer assembly and cross-linking [14], [15]. The latter provides high protein stability with strong protein linkage to the surface, but it may result in a decrease of enzymatic activity [16].

Few papers report on PEDOT used as conducting component for amperometric glucose sensing with crosslinked agents [9], [17]. Kakhki *et al.* [9] studied cross-linking of poly(methylene blue) modified PEDOT layers on a glassy carbon electrode with various cross-linking agents for ascorbate and glucose sensing. They showed that the use of glutaraldehyde (GA) as cross-linker led to higher glucose sensitivity values with respect to others like glyoxal, epichlorohydrin, and carbodiimide-N-hydroxysuccinimide. Wisitsoraat *et al.* [17] reported on graphene-PEDOT:polystyrene sulfonic acid (GP-PEDOT:PSS) modified screen-printed carbon electrode for electrochemical detection of glucose with a sensitivity of  $7.23 \mu\text{A}/\text{mM}$  narrow linear dynamic range of 20-900  $\mu\text{M}$ . However, the development of cross-linked PEDOT-bioreceptor interfaces for continuous glucose monitoring still remains a challenge.

The integration of the biosensing device with sensor AFE and electronics may allow accurate measurement, processing and wireless communication of the acquired data, paving the way toward multi-functional electronic systems that embed (bio)chemical sensors, microfluidics, and biocompatible materials for POC applications. Several design options for sensor AFE, data acquisition, and signal processing are possible [18].

Potentiostat circuits are widely adopted in electrochemical sensors read-out for glucose monitoring devices in diabetes management applications [19]. Different architectures for the implementation of a potentiostat circuit are generally used, depending on the specific use-case: for instance, most architectures work with unidirectional currents, from either reduction or oxidation reaction occurring at the working electrode, others are best suited for low power consumption, or to achieve relatively high signal to noise ratio, etc. [20]. Three-electrode electrochemical sensors have been reported, coupled with electronic circuits in order to build a system with conditioning and read-out functionalities [21].

In this work, we show a novel glucose-sensing device consisting of a planar three-electrode system on a flexible plastic foil coupled with a conditioning, read-out, and interface electronics which operates to measure glucose concentration in the blood clinical range. The working electrode is composed of a polyethylene terephthalate/gold (PET/Au) electrode modified by electropolymerization of 3,4-ethylenedioxythiophene (EDOT), followed by cross-linking immobilization of glucose oxidase via glutaraldehyde bifunctional linkers. The amperometric biosensor is integrated with a versatile circuit architecture, suitable to detect both oxidation and reduction currents and which allows low power consumption for wireless-powered applications. At the same time, it gives a

good read-out accuracy and low limit of detection (LOD), guaranteed by the low offset voltage of the operational amplifiers. Furthermore, we report the design and development of a wireless-powered system in which the potentiostat plays a crucial role in the sensor conditioning and interfacing. Finally, in order to investigate the feasibility of the application of Fluctuation Enhanced Sensing (FES) techniques [22], [23] to the amperometric sensor we developed, we designed a very low noise potentiostat; we report on the very encouraging results we have obtained, that may be regraded as a first step toward the realization of future generation, highly sensitive and selective sensor systems.

## II. MATERIALS AND METHODS

### A. Chemicals

Anhydrous D-glucose (VWR Chemicals),  $\text{AgNO}_3$  (J.T. Baker), ferrocene and phosphate buffer solution (PBS, pH 7.4) (both Alfa Aesar) were used as received. 3,4-Ethylenedioxythiophene (97%),  $\text{LiClO}_4$  (97%), Glucose oxidase (GOx; from *Aspergillus niger* Type VII, lyophilized powder,  $\geq 100,000$  units/g, solid), ascorbic acid, glutaraldehyde (25%), acetonitrile, NaCl, KCl,  $\text{HNO}_3$ , and ethanol were purchased from Sigma Aldrich and used without further purification.

### B. Electrochemical Apparatus

Electrochemical electrode depositions were performed with a Potentiostat/Galvanostat (Metrohm Autolab PGSTAT 128N) using two different cell electrode modes. The two-electrode mode was used for the electrochemical preparation of quasi-reference electrode (RE), where graphite rod was used as counter electrode and gold layer evaporated onto PET substrates was used as working electrode, respectively.

Three electrode mode was used for sensor working electrode fabrication, where graphite, Ag/AgCl (3.5 M KCl, Hanna Instruments) and gold layers were used as a counter, reference, and working electrodes, respectively. All potentials were reported with respect to Ag/AgCl (3.5 M KCl) reference electrode unless otherwise indicated. Sensor electrochemical measurements were performed with electronics designed in this work.

### C. Sensor Microfabrication

The amperometric planar electrode platform used in the present study consisted of the rectangular working electrode (WE;  $2 \text{ mm} \times 18 \text{ mm}$ ) placed in between quasi-reference electrode ( $2 \text{ mm} \times 18 \text{ mm}$ ) and the L-shaped counter electrode (CE; long arm: 22 mm; short arm: 7 mm; width: 2 mm) deposited onto the flexible PET substrates [24]–[26]. The dimensions were chosen so as to reach a compromise between the fabrication method we exploited and the noise generated by these electrodes. Indeed, the electrodes are large enough to be fabricated by evaporating gold through a shadow mask available from a laboratory workshop. However, they are also small enough to provide the best sensor stability and lower current noise. Moreover, we kept the working electrode area at ca.  $10 \text{ mm}^2$ . In fact, as Kuberský *et al.* [27] reported, increasing the working electrode area above  $15 \text{ mm}^2$ , doubling the size

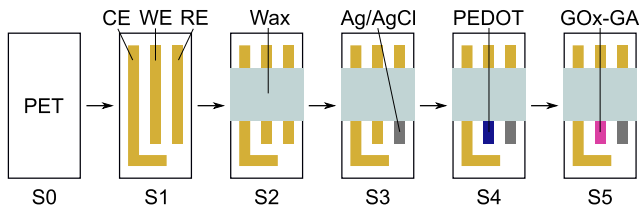


Fig. 1. Multi-step preparation of electrodes. S0: a flexible PET slab is cut in the desired dimensions ( $15 \text{ mm} \times 25 \text{ mm}$ ). S1: using a custom mask, Au vapor is deposited to form 3 electrodes, namely counter electrode (CE), working electrode (WE) and quasi-reference electrode (RE). S2: paraffin wax is applied to separate the active sensor area. S3: Ag (and then AgCl) are electrodeposited over RE. S4: PEDOT is electropolymerized onto WE. S5: GOx is cross-linked via GA onto PEDOT.

causes a threefold increase in the generation-recombination noise, and decreases the stability of the sensor. Hence, the smaller the electrode area, the better the stability of the sensor and the lower the noise level. The fabrication procedure is illustrated in Fig. 1.

Prior to Au vapor deposition, the PET substrates ( $15 \text{ mm} \times 25 \text{ mm}$ ) were ultrasonically cleaned using acetone and distilled water for 5 min (each bath); see Fig. 1, S0. To fabricate electrode template, gold metal layers (50 nm) were patterned onto PET support by vacuum evaporation through a shadow mask using high purity gold (99.9985%, Alfa Aesar) in a K975X Turbo Evaporator (Quorum Technologies) under vacuum ( $10^{-5}$  mbar); Fig. 1, S1. After the gold deposition, a thin layer of paraffin wax was deposited onto the platform to separate electrode contact area from working area, leaving an active area of the WE of  $0.1 \text{ cm}^2$ .

To fabricate quasi-reference Au/Ag/AgCl electrode, Fig. 1, S3, Ag electroplating was performed from 0.3 M  $\text{AgNO}_3$  solutions in 0.1 M  $\text{HNO}_3$  by applying a constant voltage at  $-0.9 \text{ V}$  for 600 s, followed by electrochemical chloridization in 0.5 M  $\text{NaCl}$  solution by applying a constant voltage of  $0.5 \text{ V}$  [28].

The electropolymerization of PEDOT was then carried out at room temperature in 0.01 M EDOT monomer solution and 0.01 M  $\text{LiClO}_4$  as counter ion in acetonitrile, selectively plating the exposed surface of WE (Fig. 1, S4). Polymerization was achieved applying a fixed potential of  $1.4 \text{ V}$  (referred to as polymerization potential) vs. Ag/AgCl for a period of ca. 120 s. Prior to enzyme immobilization,  $2 \mu\text{L}$  of 10 mM ferrocene in ethanol was deposited onto the reaction region of the electrode surface and then the electrodes were dried at room temperature. In our setup, ferrocene acts as a mediator between PEDOT and GOx. The enzyme immobilization was achieved by cross-linking of GOx with GA onto PEDOT. For the enzyme immobilization,  $100 \mu\text{L}$  of GOx enzyme solution ( $50 \text{ mg/mL}$ ) in 0.1 M PBS (pH 7.4) was mixed with  $20 \mu\text{L}$  of 2.5% v/v GA cross-linking solution. The mixed solution ( $5 \mu\text{L}$ ) was then dropped on PEDOT layer and allowed to adsorb and dry in air at room temperature for one hour. After immobilization, the sensors were mildly washed with PBS (Fig. 1, S5).

#### D. Electronics

An STM8L microcontroller and the operational amplifiers of the TSV71x family, characterized by a low offset

voltage ( $<200 \mu\text{V}$ ), low power consumption ( $<10 \mu\text{A}$  per channel) and  $150 \text{ kHz}$  bandwidth, were selected to implement the potentiostat circuit and its digital interface.

The electronic setup also included a dual interface EEPROM (DI EEPROM) NFC chip, an RFID antenna, and the NFC reader, respectively M24LR16E on an M24LR-discovery board and a CR95HF demo board. All parts are available as off-the-shelf components provided by STMicroelectronics.

#### E. Implemented Biosensor Electronics

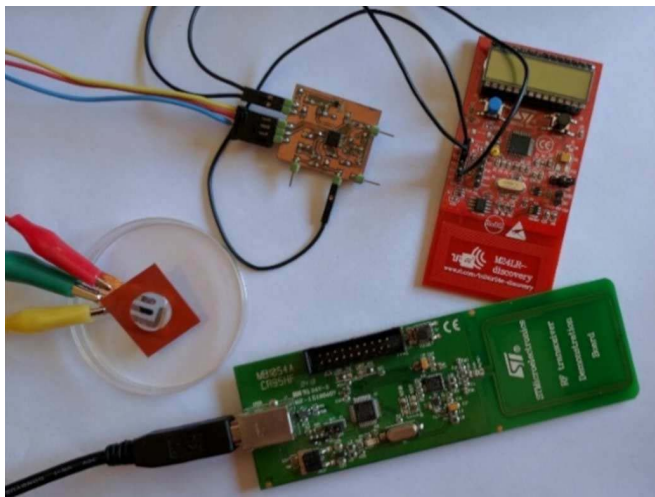
The sensor was integrated with a conditioning, read-out, and interfacing system (Fig. 2), while the whole electronic system is composed of the following modules

1) *The Sensor AFE*: With the readout and conditioning circuit (potentiostat) [18], [29], [30]. Upon accurate characterization of the electrochemical sensor, we designed a bespoke potentiostat to fit the specific sensor electrical parameters. Through a regulator and a voltage reference (Fig. 2, c and d), the circuit is able to fix the potential difference between working and reference electrodes to  $350 \text{ mV}$ , while the amperometric current assessed at the working electrode is converted to a voltage through the transimpedance amplifier in Fig. 2, e, first, and conditioned to fit the inputs requirement of the digital microcontroller, then (Fig. 2, f). The value of  $350 \text{ mV}$  was chosen as a potential difference between working and reference electrodes as reported in the literature for PEDOT-modified glucose sensors [31].

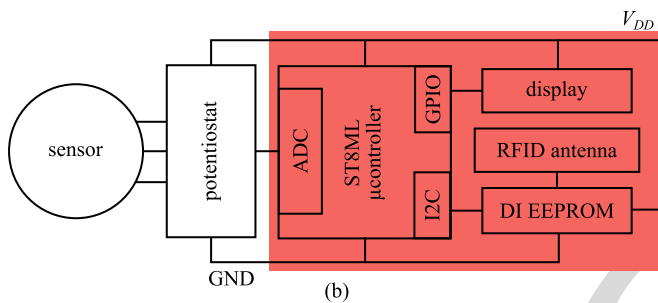
The operational amplifier U1 provides a virtual ground reference voltage to the circuit: the corresponding value is half of the supply voltage,  $V_{DD}/2$ , at the node ZERO, by means of two identical resistors connected to the non-inverting input of U1. This virtual ground voltage ZERO is used both by the device U6 (Fig. 2, d), to establish a precise reference voltage, and as the virtual ground voltage at the non-inverting input of the transimpedance amplifier U2 (Fig. 2, e). In Fig. 2, d, the device U6 provides a  $1.225 \text{ V}$  reference voltage, while the resistors  $R_1$ ,  $R_2$ , and  $R_3$  allow to establish a fixed potential difference of  $350 \text{ mV}$  between the potential of the virtual ground (ZERO) and the non-inverting input of the operational amplifier U3 corresponding to the value of the potential difference between the electrochemical cell potential and the reference electrode.

This circuit configuration (grounded working electrode) ensures that the potential of the working electrode (WE), connected to the inverting input of the operational amplifier U2 (via resistor  $R_{WE}$ ), is fixed to the ZERO voltage, while the potential at the reference electrode (RE), connected to the inverting input of the operational amplifier U3, is maintained at a value  $350 \text{ mV}$  lower than the WE potential. The output signal of the system is obtained from the node  $V_{OUT}$ . Through the transimpedance amplifier block of Fig. 2, e, the amperometric current signal generated by the sensor flows through the resistors  $R_{WE}$  ( $50 \Omega$ ) and  $R_{TIA}$  ( $100 \text{ k}\Omega$ ) and is converted into a voltage. Fig. 2, f, shows a simple voltage level shifter, as needed to adapt the generated voltage levels to the input range of the microcontroller ADC peripheral. The same block includes a simple RC low pass filter in order to filter the noise and smooth the signal.

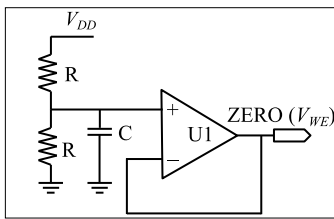




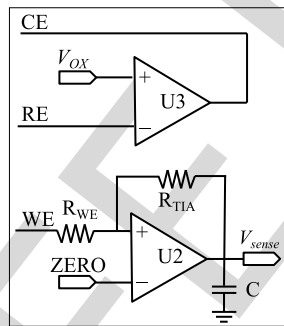
(a)



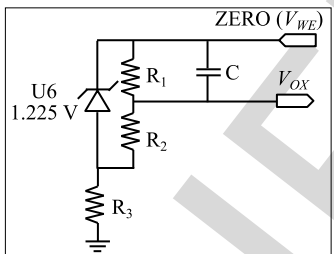
(b)



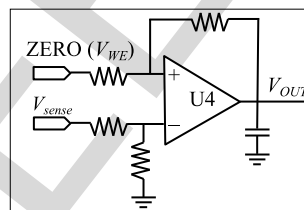
(c)



(e)



(d)



(f)

Fig. 2. Implemented electronics for the biosensor. (a) Photo of used system circuit with sensor (left) connected to the custom potentiostat (orange, center), digital control module M24LR-discovery board, with NFC and LCD (red) and NFC reader CR95HF (green). (b) Block diagram of the system; in red, the components integrated into the M24LR-discovery board. (c) Virtual zero voltage reference circuit;  $R = 1 \text{ M}\Omega$ , U1: operational amplifier,  $V_{DD}$ : supplied voltage. (d)  $V_{OX}$  voltage reference circuit (350 mV lower than the virtual zero voltage);  $R_1 = 300 \text{ k}\Omega$ ,  $R_2 = 750 \text{ k}\Omega$ ,  $R_3 = 4.7 \text{ k}\Omega$ . (e) U2: transimpedance amplifier (TIA) circuit, U3: potentiostat circuit,  $R_{WE} = 50 \Omega$ ,  $R_{TIA} = 100 \text{ k}\Omega$ . (f) Voltage level shifter. For all circuits,  $C = 100 \text{ nF}$ . (c) through (f) form the custom potentiostat showed in the photo (a) (orange).

277

278

2) *The Digital Control Module:* With NFC and LCD. This part of the system converts the output of the Sensor AFE

by means of an ADC, processes, and stores the data in the Dual Interface EEPROM, and shows the results on a display. The portable system ADC has a 12 bit resolution which, for the range we used, means having a resolution on the output voltage of 1.24 mV. The ADC clock is programmable between 320 kHz and 16 MHz (default 16 MHz). The shortest conversion time for a 12-bit resolution is  $1 \mu\text{s}$ . Each conversion step (which consists of switching the capacitor network, comparing results, and storing them to a register bit) is performed in on ADC clock cycle. Consequently, a 12-bit conversion takes 12 cycles. The sampling period has a programmable range from 4 to 384 clock cycles [32]. The frequency at which a measurement is performed and stored in the EEPROM memory is programmable. Given the slow dynamics of the glycemetic trend in humans, we have chosen a default value of 4 measures per second. The Dual Interface EEPROM includes an NFC energy harvesting for both power supply and wireless communication [30], [33]. In particular, the system consists of a bespoke potentiostat, a microcontroller (STM8L) programmed for A/D conversion, data processing, and management of both the LCD display and the dual interface EEPROM NFC chip (M24LRxxE) via I2C.

3) *The NFC Reader CR95HF and RFID Antenna Module:* Providing means to i) transfer the acquired data wireless from the digital control module to the NFC reader and from the reader to a PC via USB; ii) program the Dual Interface EEPROM NFC chip; and iii) power supply wireless both the Sensor AFE and the Digital Control module, including the NFC chip and LCD display. More in details, in the Sensor AFE module, the potentiostat circuit consisting of three operational amplifiers provides high sensor stability and optimal accuracy [34]. An additional operational amplifier is used as voltage level shifter. Therefore, we designed the sensor AFE using the quad operational amplifiers package TSV714 (STMicroelectronics).

In order to test the potentiostat, the circuit was connected to a power supply and the analog output was connected to a data acquisition board programmed to record the behavior of the signal coming from the sensor, with a high sampling rate. The above complex system allowed to monitor the concentration of glucose by chronoamperometry. The Microcontroller firmware is programmed to monitoring the voltage at the output pin of the potentiostat circuit through the 12 bit ADC peripheral. The internal clock and one of the internal timers of the microcontroller are configured to trigger the ADC in order to periodically start A/D conversions using a Direct Memory Access (DMA).

#### F. Low Noise Potentiostat for FES Noise Measurements

Fluctuation Enhanced Sensing (FES) is a sensing approach in which the noise superimposed to the DC response is taken as the relevant signal. Indeed, it has been shown that the behavior of the low frequency noise produced by a sensor depends, for the same DC reponse, on the nature of the chemical species interacting with the sensor. While a single sensor electronic nose based on FES as hypothesized in [22] is yet to be demonstrated, it is apparent that FES may allow increasing the selectivity of the sensor so as to distinguish in between

279  
280  
281  
282  
283  
284  
285  
286  
287  
288  
289  
290  
291  
292  
293  
294  
295  
296  
297  
298  
299  
300  
301  
302  
303  
304  
305  
306  
307  
308  
309  
310  
311  
312  
313  
314  
315  
316  
317  
318  
319  
320  
321  
322  
323  
324  
325  
326  
327  
328  
329  
330  
331  
332  
333  
334  
335

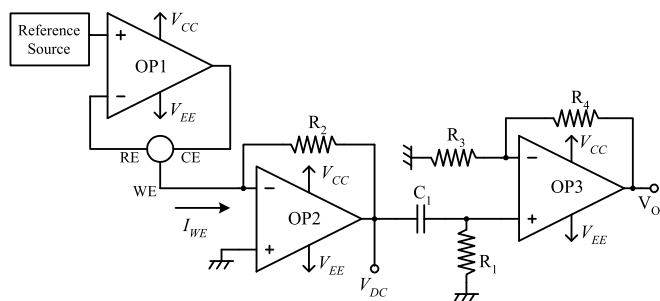


Fig. 3. Low noise potentiostat for FES measurements. Noise spectra are estimated at output  $V_O$ . Output  $V_{DC}$  is used to monitor the DC response.

the same DC response due to competing interferents. For FES experiments to be possible, it is mandatory to minimize the noise introduced by the instrumentation and the interferences coming from the environment. The low noise potentiostat we have designed for FES experiments on the developed devices is reported in Fig. 3. The reference source, based on the ultra low noise voltage reference in [35], together with the operational amplifier OP1 is used to set the potential of the reference electrode RE to the desired value (with respect to the electrode WE). The current through the working electrode WE is at the input of a low noise, DC coupled transresistance amplifier (OP2 and  $R_2$ ) and the value of the DC component of  $I_{WE}$  can be monitored through the output  $V_{DC}$ . The fluctuations are further amplified by an AC coupled amplifier stage (OP3) for the estimation of the current noise spectrum at the WE. The system is maintained in an aluminum box that acts as an electromagnetic shield. Two BNCs are available for connecting the outputs  $V_{DC}$  and  $V_O$  to the acquisition system based on a Dynamic Signal Analyzer (DSA) board by National Instruments (NI-4462).

#### G. X-Ray Photoelectron Spectroscopy (XPS)

In order to characterize the chemical nature of the sensor surface [36], [37], XPS analysis was performed by means of a PHI 5000 VersaProbe II spectrometer (ULVAC-PHI), equipped with a monochromatic Al  $K\alpha$  X-ray source ( $h\nu = 1486.6$  eV). XPS spectra were collected at a  $45^\circ$  photoelectron take-off angle.

Single elements narrow region scans were recorded, namely C 1s, S 2p, Cl 2p, and N 1s, using a  $100 \mu\text{m}$  diameter, 25 W, 15 kV beam, 23.50 eV pass energy, energy resolution 0.050 eV. The XPS spectra were analyzed with PHI MultiPak 9.6.1.7 Software, using a Shirley background and Gauss-Lorentz or asymmetric Doniach-Šunjić line shapes. All binding energies values were referred to C 1s adventitious carbon peak (284.80 eV).

#### H. Glucose Detection Measurements

A fresh stock solution of 0.1 M D-glucose was prepared in 0.1 M PBS at pH 7.4 24 h before use, to permit equilibration of  $\alpha$  and  $\beta$  anomers of D-glucose. The sensor was inserted in an incubation chamber (CoverWell™ Incubation chamber, Grace Bio-Labs) in order to perform electrochemical measurements. Amperometric determination of the biosensor

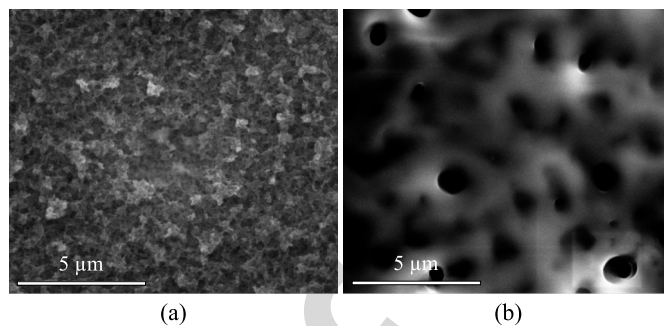


Fig. 4. SEM images of PEDOT surfaces before (a) and after (b) glucose oxidase immobilization, showing complete coverage of the surface.

response was achieved in a reaction cell containing 200  $\mu\text{L}$  PBS (50 mM, pH 7.4) and 0.1 M KCl with and without glucose, by applying constant potential at 0.35 V at 25  $^\circ\text{C}$ . After the background current reached a steady state, the drop would be aspirated and the new portion of 200  $\mu\text{L}$  of PBS with high glucose concentration (increment step: 2 mM) was deposited (by micropipette) onto the working surface of the sensor and then the current change was monitored.

#### I. Scanning Electron Microscopy (SEM)

SEM images were obtained using FEI FEG-ESEM (mod. QUANTA 200) at 12 kV and 10000 $\times$  magnification.

### III. RESULTS AND DISCUSSION

#### A. Cross-Linked-GOx/PEDOT Working Biosensor Interface

The surface morphologies of the as-prepared electropolymerized PEDOT with and without GOx cross-linked by glutaraldehyde were characterized by SEM. Fig. 4, a, shows a typical SEM image of the electropolymerized PEDOT film having a three-dimensional porous structure (200-600 nm pore size) which makes it suitable for bioreceptor immobilization. Indeed, after the deposition of GOx-GA, a thick, densely packed protein layer with voids having a diameter of ca. 200-900 nm completely obscures the underlying PEDOT morphology (Fig. 4, b). A similar morphology was observed by Buber *et al.* for cross-linked GOx on polymer surfaces [38].

In order to investigate the chemical composition of the as-prepared electrodeposited PEDOT and GOx-modified PEDOT films, XPS was employed. As expected, a preliminary XPS survey (not shown) of the electrodeposited PEDOT showed the presence of C, S, O, Cl, while, by comparison, the same polymer after the protein immobilization showed only C, N, O, and S in very low amount, indicating a good coverage of the PEDOT surface by GOx. The C 1s, N 1s, S 2p and Cl 2p regions analysis results are summarized in Table I, reporting found binding energies (BE) and relative atomic abundance expresses as atomic percentage (at%).

The C1 s spectrum of PEDOT (Fig. 5, a) shows six different peaks, three assigned to PEDOT (C-S, C = C-O, C-C-O, in a 1:1:1 ratio), the C-C/C-H and C = O ascribed to ubiquitous adventitious carbon moieties and a shake-up band [39]. The S 2p spectrum (Fig. 5, c) shows the S 2p<sub>3/2</sub> - S 2p<sub>1/2</sub> peaks with values characteristic for PEDOT [39], while the Cl 2p spectrum (Fig. 5, e) shows only a species with usual

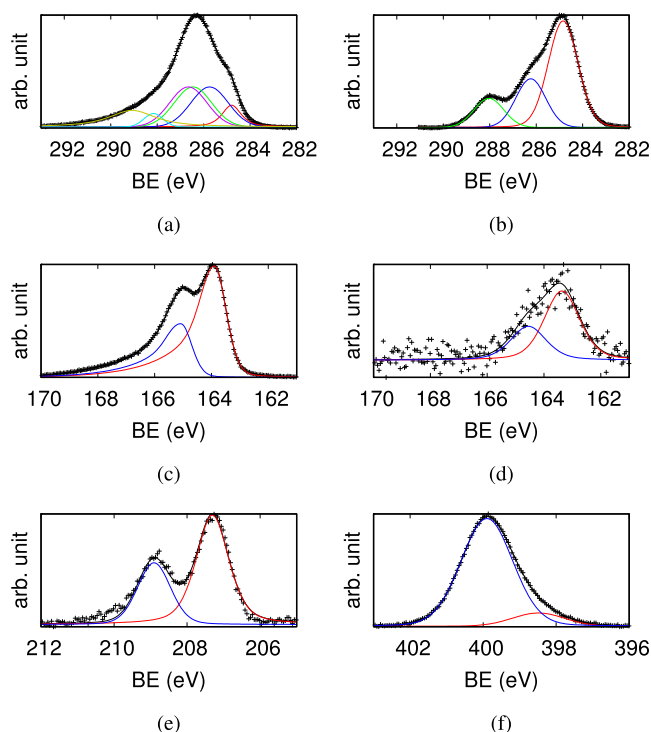


Fig. 5. XPS C 1s (a), S 2p (c) and Cl 2p (e) regions of PEDOT surfaces; and C 1s (b), S 2p (d) and N 1s (f) of GOx-covered PEDOT surfaces.

TABLE I  
XPS ANALYSIS RESULTS BEFORE (PEDOT) AND AFTER GOX  
IMMOBILIZATION (GOX-PEDOT)

	PEDOT		PEDOT-GOx	
	BE (eV)	at%	BE (eV)	at%
C-C/C-H	284.80	59.24	284.84	72.83
C-S	285.75	-	-	-
C=C-O	286.46	-	-	-
C-O <sub>proteic</sub>	-	-	286.24	-
C-C-O	286.66	-	-	-
C=O	288.16	-	288.24	-
$\pi$ - $\pi$ *	289.08	-	-	-
S 2p <sub>3/2</sub>	163.89	9.41	163.37	0.20
S 2p <sub>1/2</sub>	165.07	-	164.55	-
Cl 2p <sub>3/2</sub>	207.31	1.29	-	-
Cl 2p <sub>1/2</sub>	208.91	-	-	-
N <sub>proteic</sub>	-	-	398.49, 399.90	12.57

3/2-1/2 splitting. The value is in line with those expected for PEDOT-LiClO<sub>4</sub> [40].

After the protein immobilization, several drastic changes were observed (Fig. 5, b, d and f). It is possible to observe the presence of N (present only in GOx) and the disappearance of Cl (embedded in electrodeposited PEDOT) elements. The binding energies of N 1s are characteristic of proteic nitrogen (399-401 eV). Also, the binding energies found for C 1s are characteristic of the C-C/C-H, C-OH and C = O groups, whereas the S 2p signals are significantly lower than those observed for PEDOT films with atomic percentages (well below 1%), and in line with the S abundance in GOx. Due to

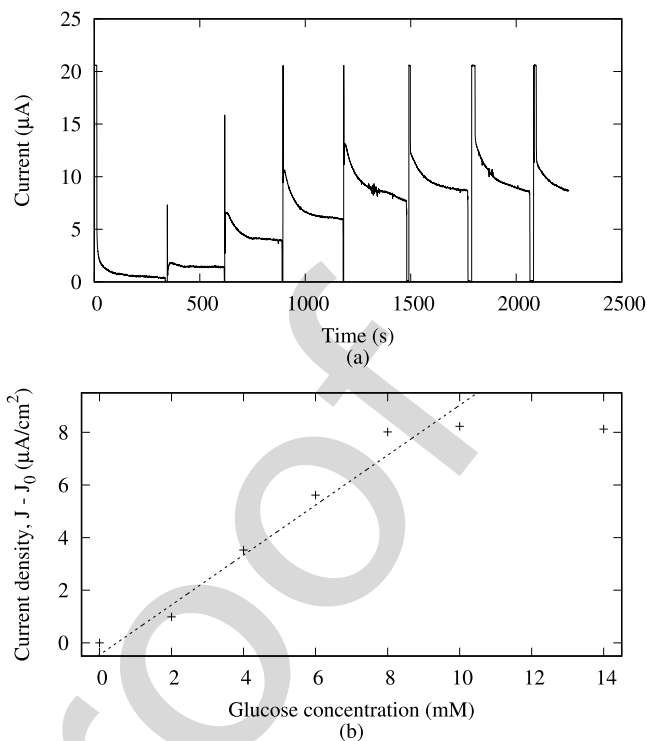
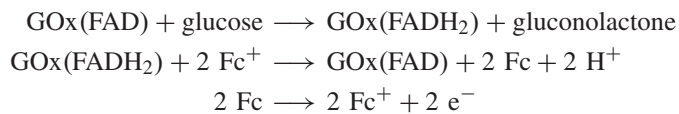


Fig. 6. Biosensor response. (a) Amperometric response; jumps correspond to drop additions. (b) Corresponding calibration curve.  $J_0$ : blank solution current density.

the strictly superficial nature of XPS analysis, all these changes give a clear evidence of a protein full coverage.

### B. Performance of the Biosensor/Potentiostat System

Amperometric responses of the biosensor coupled with potentiostat were studied at a constant applied potential of 0.35 V. Typically, in the presence of ferrocene (Fc) mediator the glucose oxidase catalyzes the oxidation of glucose to gluconolactone as follows:



In this process, the enzyme (and the enzyme redox cofactor, flavin adenine mononucleotide, FAD) is converted to its reduced form (flavin adenine dinucleotide, FADH<sub>2</sub>) [41]. After the reaction of glucose and GOx, the reduced-state of the enzyme reacts with ferricinium ion to form the oxidized-state of the enzyme and ferrocene. The reoxidized current is detected on the electrode to determine glucose concentration [31]. The biosensor exhibited a rapid and sensitive response to changes in glucose concentration, indicating the excellent electrocatalytic behavior of the PEDOT/GOx-GA biosensor. The initial current value of 0.33  $\mu\text{A}$  related to PBS is considered as a reference baseline for the successive current values. The total current as a function of the increased glucose concentration, between 0 and 14 mM is shown in Fig. 6, a. However, it is noticeable that the saturation in the detection current is clearly observed at glucose concentrations above 10 mM due to enzyme limited reactions. The biosensor showed



TABLE II  
ANALYTIC PARAMETERS COMPARISON FOR GOX-POLYMER  
MATRICES BASED GLUCOSE BIOSENSORS

Matrix	Linear range <sup>a</sup>	Sensitivity <sup>b</sup>	LOD <sup>a</sup>	Refs.
PoPD/PB/Au	0.05-10	1.25	–	[44]
GP-PEDOT:PSS	0.02-0.9	7.23	$3 \cdot 10^{-4}$	[17]
PEDOT:PSS	0.2-1.6	0.53	$10^{-2}$	[17]
SPP-PEDOT:PSS	0-10	7.57	1.16	[45]
NPG/PEDOT	0.1-15	7.3	10	[46]
PEDOT	0-10	9.24	0.1	our work

<sup>a</sup> mM <sup>b</sup>  $\mu\text{A}/(\text{mM} \cdot \text{cm}^2)$ ;

PoPD: poly(*o*-phenylenediamine); PB: Prussian Blue; GP: Graphene; PEDOT:PSS: poly(3,4-ethylenedioxythiophene) polystyrene sulfonate; SPP: sericin protein photoresist; NPG: nanoporous gold

460 the sensitivity of  $9.24 \mu\text{A}/(\text{mM} \cdot \text{cm}^2)$ , calculated as the slope  
461 value of the calibration curve (Fig. 6, b) and a detection  
462 limit (LOD) of 0.1 mM ( $\text{LOD} = 3 \cdot \sigma / \text{slope}$ ). In comparison to  
463 previously reported chemically modified electrodes, our sensor  
464 showed improved sensitivity within the linear response range  
465 (Table II).

466 To further characterize the GOx enzyme performance in  
467 the sensor, the Michaelis-Menten enzyme kinetics model  
468 was used. Therefore,  $I_{\text{max}}$  and  $K_M^{\text{app}}$  (apparent Michaelis-  
469 Menten constant) of GOx were calculated according to  
470 Anusha *et al.* [42] from:

$$471 \quad I = \frac{I_{\text{max}} \cdot [\text{glucose}]}{K_M^{\text{app}} + [\text{glucose}]}$$

472  $I_{\text{max}}$  was found to be  $17.49 \mu\text{A}$  and  $K_M^{\text{app}}$  was calculated to  
473 be 11.6 mM, smaller than the  $K_M^{\text{app}}$  reported for native glucose  
474 oxidase (33 mM) [43]. Since  $K_M^{\text{app}}$  is inversely proportional to  
475 the substrate-enzyme affinity, this implies a higher enzymatic  
476 activity of the immobilized glucose oxidase, lower diffusion  
477 barrier and higher affinity to glucose.

### 478 C. Fluctuation Enhanced Sensing Results

479 The results of low frequency noise measurements when the  
480 sensor is connected to the system in Fig. 3 are summarized  
481 in Fig. 7.

482 The spectra of the current fluctuations at the working  
483 electrode are reported in the case in which the sensor is  
484 immersed in PBS solution and for increasing concentrations  
485 of glucose. Spectral estimation is only started after about  
486 15 min when the transients following the increase of glucose  
487 concentration are extinct. As it is apparent from the figure,  
488 the level of low frequency noise is an increasing function of the  
489 glucose concentration. The dependency of the low frequency  
490 noise on the glucose concentration can be better appreciated  
491 in the inset in Fig. 7 where the square root of the noise at 1 Hz  
492 is reported vs the glucose concentration. The results suggest  
493 that the current noise spectrum generated by the interaction  
494 of the sensor with the solution is proportional to the glucose  
495 concentration squared. FES, as we have noted before, is not  
496 just supposed to be an alternative to the measurement of the  
497 DC current, but, rather, a measurement approach by which we  
498 can distinguish among chemical species interacting with the

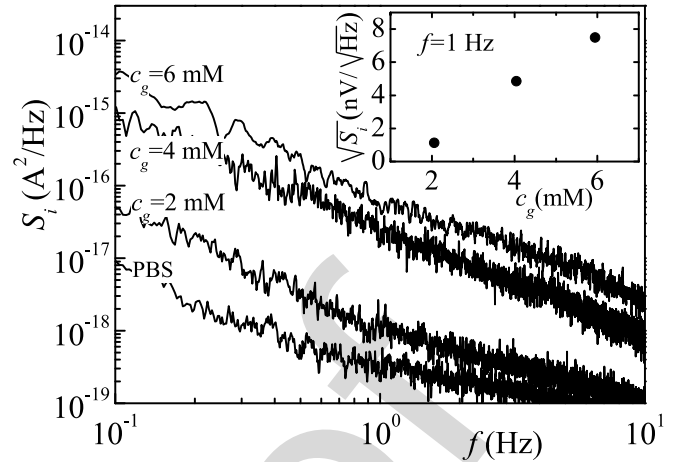


Fig. 7. Power spectral density of the current fluctuations through the working electrode in a PBS solution and for increasing glucose concentrations. The inset shows the linear dependence of the square root of the noise at ( $f = 1$  Hz) vs. the glucose concentration  $c_g$ .

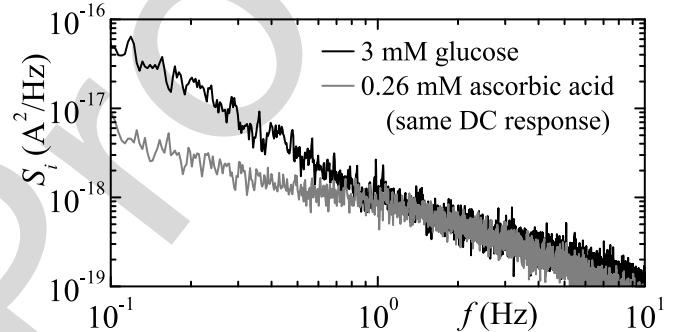


Fig. 8. Power spectral density of the current fluctuations, for the same DC response, of two sensors immersed in a glucose solution (black line) and in an ascorbic acid solution (gray line). The difference at low frequencies, clearly demonstrates that by analyzing the noise spectra it is possible to distinguish among different chemical species interacting with the sensor.

499 sensor [23]. In order to test whether the developed devices  
500 display such behavior, we repeated noise measurements on  
501 two new devices, one immersed in a 3 mM glucose solution  
502 (mid-range concentration with respect to the experiments on  
503 the sample used for Fig. 7) and another one in an ascorbic acid  
504 solution. The concentration of ascorbic acid was adjusted in  
505 such a way as to obtain the same DC response as in the case  
506 of the 3 mM glucose solution. When the measured spectra are  
507 compared (Fig. 8), it is apparent that they have, in the lower  
508 frequency portion, quite different shapes. This means that the  
509 shape of the spectrum at low frequencies can be possibly  
510 used as a marker for distinguishing among different species  
511 interacting with the sensor when there is the suspect that the  
512 DC response may be due to interferent species. This result has  
513 to be regarded as encouraging as it proves that the devices we  
514 propose are good candidates for the development of advanced  
515 approaches based on FES.

## 516 IV. CONCLUSION

517 A novel three-electrode planar flexible biosensing amper-  
518 ometric platform for glucose monitoring, having a cross-  
519 linked biointerface, coupled with a conditioning, readout, and

interfacing system have been demonstrated. The biosensor includes a simplified biochemical interface consisting of a cross-linked protein superstructure onto a conductive polymer without the addition of other expensive conductive nanostructures like carbon nanotubes and graphene oxide. Moreover, our integrated platform architecture has numerous advantages over previous developments: i) the device is low-cost and portable; ii) the electronic system has a wireless RF power supply, low power consumption, ability to store data logs of the glucose concentration; iii) the digitization of data opens the way to remote diagnostics; iv) the biosensing platform can be easily integrated with other sensors for multitasking using the same layout. Furthermore, we have shown that the devices we have developed are good candidates for the development of advanced sensing techniques based on FES.

## REFERENCES

- [1] *Global Report on Diabetes*, World Health Org., Geneva, Switzerland, 2016.
- [2] E. Layne, D. Sayler, and S. Bessman, "Continuous monitoring of blood glucose and PO<sub>2</sub> with a glucose electrode," *Fed. Proc.*, vol. 33, no. 3, p. 276, 1974.
- [3] J. Wang, "Electrochemical glucose biosensors," in *Electrochemical Sensors, Biosensors, and Their Biomedical Applications*, X. Zhang, H. Ju, and J. Wang, Eds. Norwell, MA, USA: Academic, 2008, ch. 3, pp. 57–69.
- [4] S. Libertino, S. Conoci, A. Scandurra, and C. Spinella, "Biosensor integration on Si-based devices: Feasibility studies and examples," *Sens. Actuators B, Chem.*, vol. 179, pp. 240–251, Mar. 2013.
- [5] D. G. Rackus, M. H. Shamsi, and A. R. Wheeler, "Electrochemistry, biosensors and microfluidics: A convergence of fields," *Chem. Soc. Rev.*, vol. 44, no. 15, pp. 5320–5340, 2015.
- [6] F. Ricci and G. Palleschi, "Sensor and biosensor preparation, optimisation and applications of prussian blue modified electrodes," *Biosensors Bioelectron.*, vol. 21, no. 3, pp. 389–407, 2005.
- [7] A. P. F. Turner, "Biosensors: Sense and sensibility," *Chem. Soc. Rev.*, vol. 42, no. 8, pp. 3184–3196, Apr. 2013.
- [8] J. Wang, "Glucose biosensors: 40 years of advances and challenges," *Electroanalysis*, vol. 13, no. 12, pp. 983–988, 2001.
- [9] S. Kakhki, M. M. Barsan, E. Shams, and C. M. A. Brett, "New robust redox and conducting polymer modified electrodes for ascorbate sensing and glucose biosensing," *Electroanalysis*, vol. 25, no. 1, pp. 77–84, 2013.
- [10] N. C. Sekar, S. A. M. Shaegh, S. H. Ng, L. Ge, and S. N. Tan, "A paper-based amperometric glucose biosensor developed with Prussian Blue-modified screen-printed electrodes," *Sens. Actuators B, Chem.*, vol. 204, pp. 414–420, Dec. 2014.
- [11] C. S. K. Lawrence, S. N. Tan, and C. Z. Floresca, "A 'green' cellulose paper based glucose amperometric biosensor," *Sens. Actuators B, Chem.*, vol. 193, pp. 536–541, Mar. 2014.
- [12] B. A. Kros, S. W. F. M. van Hövell, N. A. J. M. Sommerdijk, and R. J. M. Nolte, "Poly(3,4-ethylenedioxythiophene)-based glucose biosensors," *Adv. Mater.*, vol. 13, no. 20, pp. 1555–1557, 2001.
- [13] T.-P. Huynh, P. S. Sharma, M. Sosnowska, F. D'Souza, and W. Kutner, "Functionalized polythiophenes: Recognition materials for chemosensors and biosensors of superior sensitivity, selectivity, and detectability," *Prog. Polym. Sci.*, vol. 47, pp. 1–25, Aug. 2015.
- [14] C. Zhu, G. Yang, H. Li, D. Du, and Y. Lin, "Electrochemical sensors and biosensors based on nanomaterials and nanostructures," *Anal. Chem.*, vol. 87, no. 1, pp. 230–249, 2015.
- [15] G. A. Evtugyn, V. B. Stepanova, A. V. Porfireva, A. I. Zamaleeva, and R. R. Fakhruллин, "Electrochemical dna sensors based on nanostructured organic dyes/dna/polyelectrolyte complexes," *J. Nanosci. Nanotechnol.*, vol. 14, no. 9, pp. 6738–6747, 2014.
- [16] D. D. Sabatini, K. Bensch, and R. J. Barmett, "Cytochemistry and electron microscopy. The preservation of cellular ultrastructure and enzymatic activity by aldehyde fixation," *J. Cell Biol.*, vol. 17, pp. 19–58, Apr. 1963.
- [17] A. Wisitsoraat *et al.*, "Graphene-PEDOT:PSS on screen printed carbon electrode for enzymatic biosensing," *J. Electroanal. Chem.*, vol. 704, pp. 208–213, Sep. 2013.
- [18] J. P. Villagrasa, J. Colomer-Farrarons, and P. Miribel-Català, "Bioelectronics for amperometric biosensors," in *Bioelectronics for Amperometric Biosensors*, T. Rincken, Ed. Rijeka, Croatia: InTech, 2013, ch. 10.
- [19] M. Roknsharifi, S. K. Islam, K. Zhu, and I. Mahbub, "A low power, highly stabilized three electrode potentiostat for biomedical implantable systems," *Analog Integr. Circuits Signal Process.*, vol. 83, no. 2, pp. 217–229, 2015.
- [20] W. Y. Chung, A. C. Paglinawan, Y. H. Wang, and T. T. Kuo, "A 600  $\mu$ W readout circuit with potentiostat for amperometric chemical sensors and glucose meter applications," in *Proc. IEEE Conf. Electron Devices Solid-State Circuits*, Dec. 2007, pp. 1087–1090.
- [21] E. Lauwers, J. Suls, W. Gumbrecht, D. Maes, G. Gielen, and W. Sansen, "A CMOS multiparameter biochemical microsensor with temperature control and signal interfacing," *IEEE J. Solid-State Circuits*, vol. 36, no. 12, pp. 2030–2038, Dec. 2001.
- [22] M. P. Trawka *et al.*, "UV-light-induced fluctuation enhanced sensing by WO<sub>3</sub>-based gas sensors," *IEEE Sensors J.*, vol. 16, no. 13, pp. 5152–5159, Jul. 2016.
- [23] J. M. Smulko, M. Trawka, C. G. Granqvist, R. Ionescu, F. Annanouch, E. Llobet, and L. B. Kish, "New approaches for improving selectivity and sensitivity of resistive gas sensors: A review," *Sensor Rev.*, vol. 35, pp. 340–347, Sep. 2015.
- [24] K. Griffiths, C. Dale, J. Hedley, M. D. Kowal, R. B. Kaner, and N. Keegan, "Laser-scribed graphene presents an opportunity to print a new generation of disposable electrochemical sensors," *Nanoscale*, vol. 6, no. 22, pp. 13613–13622, 2014.
- [25] "A biosensor for measuring concentration of biomolecules," U.S. Patent 179848, 1994.
- [26] R. E. Sabzi, F. Rasouli, and F. Kheiri, "Amperometric hydrogen peroxide biosensor based on horseradish peroxidase entrapped in titania sol-gel film on screen-printed electrode," *Amer. J. Anal. Chem.*, vol. 4, no. 11, pp. 607–615, 2013.
- [27] P. Kuberský, A. Hamáček, S. Nešpůrek, R. Soukup, and R. Vík, "Effect of the geometry of a working electrode on the behavior of a planar amperometric NO<sub>2</sub> sensor based on solid polymer electrolyte," *Sens. Actuators B, Chem.*, vol. 187, pp. 546–552, Oct. 2013.
- [28] E. T. S. G. da Silva, S. Miserere, L. T. Kubota, and A. Merkoçi, "Simple on-plastic/paper inkjet-printed solid-state Ag/AgCl pseudoreference electrode," *Anal. Chem.*, vol. 86, no. 21, p. 10531–10534, 2014.
- [29] J.-L. Lai, H.-S. Chang, T.-Y. Lin, C.-F. Tai, and R.-J. Chen, "Electrochemical enzyme-electrode biosensor for Glucose detection," in *Proc. Int. Conf. Commun., Circuits Syst. (ICCCAS)*, May 2008, pp. 1208–1212.
- [30] L. Li, W. A. Qureshi, X. Liu, and A. J. Mason, "Amperometric instrumentation system with on-chip electrode array for biosensor application," in *Proc. Biomed. Circuits Syst. Conf. (BioCAS)*, Nov. 2010, pp. 294–297.
- [31] P.-C. Nien, T.-S. Tung, and K.-C. Ho, "Amperometric glucose biosensor based on entrapment of glucose oxidase in a poly(3,4-ethylenedioxythiophene) film," *Electroanalysis*, vol. 18, nos. 13–14, pp. 1408–1415, Jul. 2006.
- [32] "Analog-to-digital converter on STM8L and STM8AL devices: Description and precision improvement techniques," STMicroelectronics, Geneva, Switzerland, Appl. Note AN3137, 2012.
- [33] S. Guan, J. Gu, Z. Shen, J. Wang, Y. Huang, and A. Mason, "Wireless powered implantable bio-sensor tag system-on-chip for continuous glucose monitoring," in *Proc. IEEE Biomed. Circuits Syst. Conf. (BioCAS)*, Nov. 2011, pp. 193–196.
- [34] P. Sennequier, "Signal conditioning for electrochemical sensors," STMicroelectronics, Geneva, Switzerland, Appl. Note AN4348, 2017.
- [35] G. Scandurra, G. Giusi, and C. Ciofi, "A very low noise, high accuracy, programmable voltage source for low frequency noise measurements," *Rev. Sci. Instrum.*, vol. 85, no. 4, p. 044702, 2014.
- [36] N. R. Mohamad, N. H. C. Marzuki, N. A. Buang, F. Huyop, and R. A. Wahab, "An overview of technologies for immobilization of enzymes and surface analysis techniques for immobilized enzymes," *Biotechnol. Biotechnol. Equip.*, vol. 29, no. 2, pp. 205–220, Mar. 2015.
- [37] E. Mazzotta, S. Rella, A. Turco, and C. Malitesta, "XPS in development of chemical sensors," *RSC Adv.*, vol. 5, p. 83164–83186, Sep. 2015.
- [38] E. Buber, M. Kesik, S. Soylemez, and L. Toppare, "A bio-sensing platform utilizing a conjugated polymer, carbon nanotubes and PAMAM combination," *J. Electroanal. Chem.*, vol. 799, pp. 370–376, Aug. 2017.
- [39] V. Figà *et al.*, "Symmetric naphthalenediimidequaterthiophenes for electropolymerized electrochromic thin films," *J. Mater. Chem. C*, vol. 3, pp. 5985–5994, May 2015.



- 664 [40] S. A. Spanninga, D. C. Martin, and Z. Chen, "X-ray photoelectron spectroscopy study of counterion incorporation in poly(3,4-  
665 ethylenedioxythiophene)," *J. Phys. Chem. C*, vol. 113, no. 14,  
666 pp. 5585–5592, 2009.
- 668 [41] S. Vaddiraju, D. J. Burgess, I. Tomazos, F. C. Jain, and  
669 F. Papadimitrakopoulos, "Technologies for continuous glucose monitoring:  
670 Current problems and future promises," *J. Diabetes Sci. Technol.*,  
671 vol. 4, no. 6, pp. 1540–1562, 2010.
- 672 [42] J. Anusha, C. J. Raj, B.-B. Cho, A. T. Fleming, K.-H. Yu, and B. C. Kim,  
673 "Amperometric glucose biosensor based on glucose oxidase immobilized  
674 over chitosan nanoparticles from *gladius of Uroteuthis duvauceli*," *Sens.*  
675 *Actuators B, Chem.*, vol. 215, pp. 536–543, Aug. 2015.
- 676 [43] J. Park, H. K. Kim, and Y. Son, "Glucose biosensor constructed from  
677 capped conducting microtubules of PEDOT," *Sens. Actuators B, Chem.*,  
678 vol. 133, no. 1, pp. 244–250, 2008.
- 679 [44] C. Deng *et al.*, "New glucose biosensor based on a poly(o-  
680 phenylenediamine)/glucose oxidase-glutaraldehyde/Prussian blue/Au  
681 electrode with QCM monitoring of various electrode-surface  
682 modifications," *Anal. Chim. Acta*, vol. 557, nos. 1–2, pp. 85–94,  
683 2006.
- 684 [45] R. K. Pal, A. A. Farghaly, C. Wang, M. M. Collinson, S. C. Kundu, and  
685 V. K. Yadavalli, "Conducting polymer-silk biocomposites for flexible  
686 and biodegradable electrochemical sensors," *Biosensors Bioelectron.*,  
687 vol. 81, pp. 294–302, Jul. 2016.
- 688 [46] X. Xiao, M. Wang, H. Li, and P. Si, "One-step fabrication of  
689 bio-functionalized nanoporous gold/poly(3,4-ethylenedioxythiophene)  
690 hybrid electrodes for amperometric glucose sensing," *Talanta*, vol. 116,  
691 pp. 1054–1059, Nov. 2013.

692 **Yana Aleeva** received the B.Sc. and M.Sc. degrees in chemical technology and  
693 biotechnology from Kazan State Technological University, Russia, in 2006 and  
694 2008, respectively, the M.Sc. degree in polymer science and engineering  
695 from London Metropolitan University, U.K., in 2007, and the Ph.D. degree  
696 in nanoscience from the Scuola Superiore, University of Catania, in 2012.  
697 Since 2013, she has been a Post-Doctoral Researcher with the Department of  
698 Physics and Chemistry, University of Palermo. Her current research interests  
699 include nanomaterials for sensing applications and organic-based coatings for  
700 corrosion protection of cultural heritage.

AQ:4



**Giovanni Maira** graduated in electronics engineering from the University of Catania, Italy. He received a postgraduate specialization in nanotechnology and sustainable energies focusing his work on characterization of sensors and application specific integrated circuit for flexible and disposable electronics from the University of Palermo, Italy, and the Ph.D. degree in material science and nanotechnologies from the University of Catania in 2017, funded by the Italian National Research Council, Institute of Microelectronics and Microsystems, focusing on optical biosensors. From 2013 to 2016, he collaborated with the Department of Physics and Chemistry, University of Palermo, as a Research Support Engineer, and supported design and engineering work to large companies (e.g., STMicroelectronics) and various SMEs.

AQ:5



**Michelangelo Scopelliti** received the M.Sc. degree in 2000 and the Ph.D. degree in chemistry in 2004. Since 2010, he has been with Palermo University as Unit Director of the Inter-University Research Consortium on Metal Chemistry in Biological Systems (CIRCMSB). He has noteworthy experience with Mössbauer Spectroscopy, especially with  $^{119}\text{m}\text{Sn}$ . He is currently an Assistant Professor of Inorganic Chemistry with the Physics and Chemistry Department, Università degli Studi di Palermo. His track record includes over 70 publications in journals, conference proceedings and book chapters. His research interests go from bioinorganic chemistry (especially organotin chemistry) to spectroscopic applications, with emphasis on XPS applications to photovoltaic and sensor devices characterization.



**Vincenzo Vinciguerra** graduated in physics in 1997 and received the Ph.D. degree in materials science from the University of Catania, Italy. He joined STMicroelectronics in 2001 as a Researcher, contributing to the developments of post-silicon technologies, in EU and Singapore funded projects, and also as a PI. During his career, he carried out leading work, with main contributions in the fields of Si-photonics nanotechnology, carbon related nanomaterials (nanotubes and graphene), organic thin film devices (e.g., transistors, memories, and sensors), and smart flexible sensors. He is also an accomplished organizer/co-organizer, a reviewer, and a program committee member of specific technical events and conferences (e.g., Summer School CONTEST ITN MSCF, IEEE NANO 2015, and IEEE Prime 2015–2018). His scientific and technical activity is recorded in over 50 among patents, peer reviewed journal articles, and conference proceedings, resulting in a Scopus *h*-index of 11, with over 1170 citations.

**Graziella Scandurra** received the master's degree in electronic engineering and the Ph.D. degree in information technology from the University of Messina, in 2001 and 2005, respectively. She is currently a Researcher with the Dipartimento di Ingegneria, University of Messina. Her current research interests include the design of dedicated and low-noise instrumentation and the characterization, and the reliability of electron devices.

**Gianluca Cannatà** received the degree in electronic engineering and the Ph.D. degree in information technology from the University of Messina, Messina, Italy, in 2003 and 2008, respectively. He was a Contract Researcher with the Dipartimento di Ingegneria, University of Messina, until 2017. His research interests include the design of dedicated and low-noise instrumentation.

**Gino Giusi** received the Ph.D. degree in electronic engineering from the University of Messina, Italy, in 2005. In 2007, he joined the University of Calabria, Italy. Since 2011, he has been a Researcher and a Professor with the University of Messina. His main research interests include the study of electrical characterization techniques and reliability for solid state electronic devices, the modeling and simulation of nanoscale CMOS transistors and memories, and the design of ultra-low noise electronic instrumentation and techniques for low-frequency noise measurements.

**Carmine Ciofi** graduated *magna cum laude* in electronic engineering from the University of Pisa. He received the Ph.D. degree from the Scuola Superiore Sant'Anna. After receiving his Ph.D., he was a Researcher in electronics at the University of Pisa. In 1998, he moved to the University of Messina, where he is currently a Full Professor of Electronics. His research interests include the characterization of the reliability of electron devices and the design of dedicated instrumentation for low frequency noise applications.

**Viviana Figà** graduated in chemical engineering with specialization in electrochemistry from the University of Palermo in 2004, delving into subjects, such as applied electrochemistry, industrial electrochemical processes and corrosion, and protection of metals. She received the Ph.D. degree in chemical and materials engineering from the University of Palermo in 2009, refining basic and advanced electrochemical methods for materials science. She also graduated in naval engineering from the University of Napoli Federico II in 2017, discussing a dissertation about electrochemical devices as power generators onboard. She was a Professor of Applied Physical Chemistry with the Faculty of Science, University of Palermo, from 2009 to 2011. Her research interests regards the electrochemical deposition and characterization of inorganic and organic semiconductors to apply in optoelectronic devices, the study of electrode/electrolyte interfaces by means of advanced electrochemical techniques, and the fabrication and testing of electrochemical devices.

AQ:6

731  
732  
733  
734  
735  
736  
737  
738  
739  
740  
741  
742  
743  
744  
745  
746  
747  
748749  
750  
751  
752  
753  
754755  
756  
757  
758  
759  
760  
761  
762  
763  
764  
765  
766  
767768 AQ:7  
769  
770  
771  
772  
773  
774775  
776 AQ:8  
777  
778  
779  
780  
781  
782  
783  
784  
785  
786  
787  
788  
789

790  
791  
792  
793  
794  
795  
796  
797  
798  
799  
800  
801  
802  
803  
804  
805  
806  
807  
808  
809



**Luigi G. Occhipinti** received the M.Eng. degree, the C.Eng. degree in 1992, and the Ph.D. degree in 1997. He is the Deputy Director and COO with the Cambridge Graphene Centre, University of Cambridge. He is also a Principal Investigator with the Engineering Department, Cambridge University, the CEO and Director of Engineering with Cambridge Innovation Technologies Consulting Limited, and the Non-Executive Director of Zinergy UK Ltd. He has developed leading science and research in post-CMOS roadmap, heterogeneous integration, polymer and printed electronics, advanced bio-systems and molecular diagnostics, signal processing and nonlinear computation, mechanical, optical, and chemical sensors, with focus on miniaturization and smart products. His track record includes over 90 publications in journals and conference proceedings and over 60 patents. He is the author of two book chapters, and a co-editor of an Elements series by Cambridge University Press. His current research focuses on bio- and opto-electronics, sensor technologies, quantum dot and 2-D materials, flexible electronics, and nanofabrication. He has an *h*-index of 21, Citations: over 2300 (over 1484 since 2013).



**Bruno Pignataro** received the Ph.D. degree in materials science from the University of Catania in 2000, spending a period at the University of Münster, Germany. He is currently a Full Professor of Physical Chemistry with the University of Palermo. He is a Project Leader of the District of High Technology for innovation in the field of Cultural Heritages, Sicily, and a Delegate for Project Planning at the Department of Physic and Chemistry, University of Palermo and was awarded with over 5 M € in national and international projects. He has authored about 130 publications and over 180 conference communications. His research interests deals with molecular surfaces, plastic electronics, nanotechnology and biotechnology spanning from the study of self-organized organic, and hybrid and biological materials at surfaces to their application in electronic devices (transistors, photovoltaic cells, and sensors/biosensors). He edited seven books with Wiley and was on the Editorial Boards of different international journals as well as on the Editorial Scientific Board of "La Chimica e l'Industria" acting as an Editor of the issue *Critical Review*. He took different offices within the Italian Chemical Society, including Coordinator of the Italian Chemical Society He organized over 25 among conferences, workshops, and scientific competitions (including seven editions of the European Young Chemist Award).

810  
811  
812  
813  
814  
815  
816  
817  
818  
819  
820  
821  
822  
823  
824  
825  
826  
827  
828  
829  
830  
831  
832

IEEE PROCEEDINGS

## AUTHOR QUERIES

### AUTHOR PLEASE ANSWER ALL QUERIES

**PLEASE NOTE: We cannot accept new source files as corrections for your paper. If possible, please annotate the PDF proof we have sent you with your corrections and upload it via the Author Gateway. Alternatively, you may send us your corrections in list format. You may also upload revised graphics via the Author Gateway.**

AQ:1 = Please provide the expansion for “NFC.”

AQ:2 = Please confirm whether the edits made in the financial section are OK.

AQ:3 = Please confirm the title, patent no., and year for ref. [25]. Also provide the author name, month, and day.

AQ:4 = Please specify the degree name for the author “Giovanni Maira” which is received from the University of Catania.

AQ:5 = Please confirm whether the edits made in the sentence “Michelangelo Scopelliti received...” are OK.

AQ:6 = Please specify the degree name for the author “Vincenzo Vinciguerra” which is received from the University of Catania in 1997.

AQ:7 = Please specify the degree name for the author “Carmine Ciofi” which is received from the University of Pisa.

AQ:8 = Please specify the degree names for the author “Viviana Figà” received from the University of Palermo in 2004 and the University of Napoli Federico II in 2017.